Dalton Transactions

ROYAL SOCIETY OF CHEMISTRY

COMMUNICATION

View Article Online
View Journal | View Issue

Check for updates

Cite this: *Dalton Trans.*, 2025, **54**, 8050

Received 29th April 2025,
Accepted 30th April 2025

DOI: 10.1039/d5dt01008j

rsc.li/dalton

A palladium thiolate-SNS complex-catalyst for Mizoroki–Heck cross-coupling†

Saeed Ataie, Atousa Khanzadeh and R. Tom Baker *

Phosphine-free catalysts for the Mizoroki–Heck cross-coupling reaction offer significant advantages in terms of air and moisture stability. We synthesized two palladium(II) complexes featuring a thiolate-imine-thioether SNS pincer ligand: Pd(κ^2-SNS^{Me})$_2$ (Pd-1) and PdI(κ^3-SNS^{Me}) (Pd-2). Their catalytic activities were compared, with Pd-2 demonstrating excellent reactivity at a low catalyst loading of 1.5 mol%, efficiently producing olefin products across various substrates within 5 hours. Conversely, Pd-1 showed no catalytic activity due to its isomerization to a Pd(II)-N_2S_2 complex *via* imine C–C bond formation at elevated temperatures, which restricted access to coordination sites necessary for oxidative addition and alkene coordination. Heating Pd-2 with excess NEt_3 affords a Pd dithiolate tetramer, [Pd(μ-κ^3-SNS)]$_4$ *via* selective C–S bond activation.

Over the past decades, transition metal-catalyzed coupling reactions, such as the Mizoroki–Heck,[1] Suzuki–Miyaura,[2] Sonogashira,[3] Negishi[4] and Stille[5] reactions, have revolutionized synthetic organic chemistry by enabling the efficient formation of carbon–carbon bonds. These methodologies have become pivotal for accessing complex molecules in agrochemicals, pharmaceuticals, and fine chemical manufacturing.[6] Among them, the Heck reaction, independently discovered by Mizoroki[7] and Heck[8] in the 1970s, remains a cornerstone for constructing intricate molecular frameworks.

Palladium catalysis is central to the Heck reaction, owing to its unique ability to toggle between oxidation states (0 and +2) and its versatile coordination chemistry.[9] While phosphine-based ligands have traditionally dominated this field,[10] their cost, air sensitivity, and toxicity have driven the search for more sustainable alternatives.[11] In response, phosphine-free ligands—including N-, O-, and S-donor systems—have gained traction due to their stability, reduced toxicity, and cost-effectiveness.[12]

In previous work, we employed a thiolate-based SNS ligand (L1 in Scheme 1) with first row metals as catalysts for hydroboration[13–17] and azide–alkyne coupling reactions.[18] This ligand framework is air-stable, nontoxic, and synthesized from inexpensive starting materials,[19] addressing key drawbacks of phosphine ligands. Notably, the thiolate group can serve as a bridging element,[19,20] forming dinuclear compounds that can serve as stable precatalysts. Additionally, the thioether donor exhibits potential hemilabile behaviour during the catalytic cycle, assisting in the formation of active catalytic species.[17] The potential redox non-innocence of the ligand[21] further stabilizes the metal's oxidation state during catalysis, enhancing its versatility. In the Co and Fe complexes the thiolate SNS ligands undergo an intramolecular coupling, affording complexes bearing the redox non-innocent N_2S_2 ligand (Fig. 1A and B).[19,22] Thermolysis of the isolated Ni(L1)$_2$ complex also gives rise to Ni(N_2S_2) (Fig. 1C).[20,23] In this work we extend the

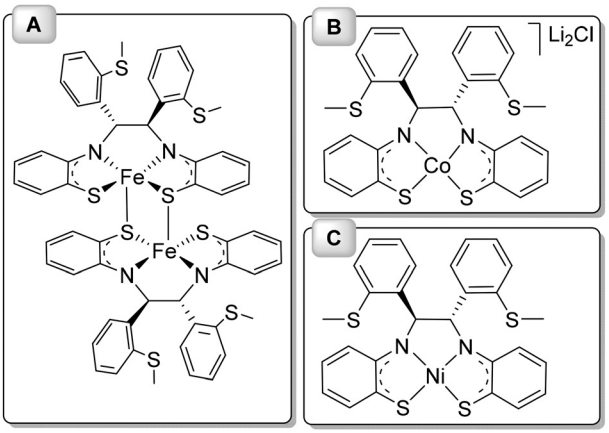

Fig. 1 [Fe(N_2S_2)]$_2$ (A), [Co(N_2S_2)][Li_2Cl] (B) and Ni(N_2S_2) (C) complexes.

Department of Chemistry and Biomolecular Sciences and Centre for Catalysis Research and Innovation, University of Ottawa, Ottawa, Ontario K1N 6N5, Canada. E-mail: rbaker@uottawa.ca

†Electronic supplementary information (ESI) available: Selected experimental, structural and spectroscopic data. CCDC 2292482, 2292483 and 2409551. For ESI and crystallographic data in CIF or other electronic format see DOI: https://doi.org/10.1039/d5dt01008j

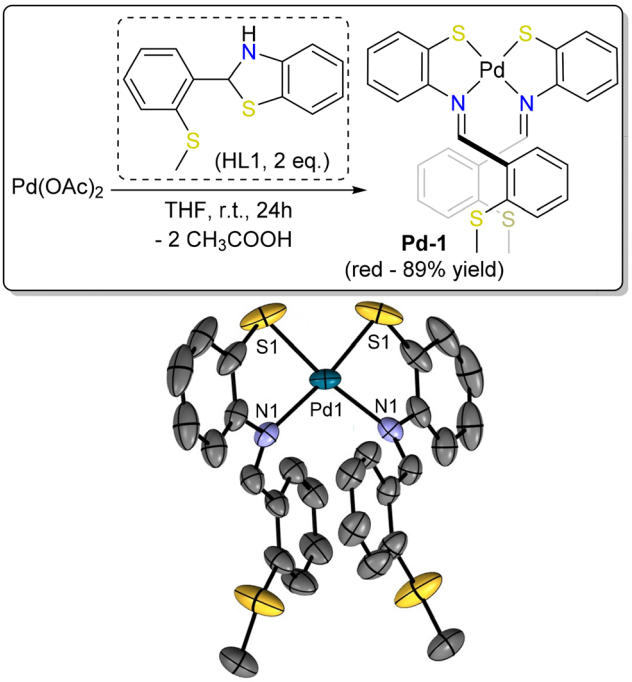

Scheme 1 Synthesis and molecular structure of **Pd-1**. The complex is centrosymmetric, with the **Pd-1** atom located on a crystallographic twofold rotation axis. Displacement ellipsoids are drawn at the 50% probability level, and all hydrogen atoms have been omitted for clarity. Selected bond distances (Å) and angles (°): Pd1–N1 = 2.090(2), Pd1–S1 = 2.2658(9), N1–Pd1–S1 = 83.39(7), N1–Pd1–N1 = 102.26(12), S1–Pd1–S1 = 91.62(6).

application of L1 to a second-row transition metal, focusing on the exploration of palladium-catalyzed Heck reactions.

The four-coordinate complex Pd(κ^2-SNS^{Me})$_2$ (**Pd-1**) was synthesized from readily available Pd(II) acetate and two equiv. of the protonated thiolate ligand tautomer (HL1; Scheme 1). The geometry of **Pd-1** exhibits a significant distortion from square-planar coordination ($\tau'4$ = 0.11), likely due to steric hindrance between the thioether groups. Nonetheless, its symmetrical structure (Pd–S1 = 2.2658(9) Å) contrasts with the Ni analog (Ni–S1 = 2.1718(7) Å and Ni–S2 = 2.1673(7) Å).[20] Moreover, the deviation from the ideal 90° angle is more pronounced in **Pd-1** [N–Pd–S = 83.397° *vs.* 86.53(6) and 86.68(6)° for N–Ni–S].

The catalytic potential of **Pd-1** was evaluated in the Heck reaction. However, **Pd-1** at 5 mol% loading produced none of the coupling product in DMF solvent after 24 hours at 120 °C. To explain the lack of catalytic activity, we anticipate the formation of Pd(N_2S_2) at elevated temperatures (Scheme 2) as discussed for Ni above.[20,23] In the generally accepted mechanism for the Heck reaction, the Pd(0) active catalyst requires two *cis* vacant sites to oxidatively add the aryl halide and a third to bind the alkene. Even if **Pd-1** were to undergo reduction to Pd (0) by the triethylamine base (*vide supra*), the rigidity of its tetradentate ligand and the resulting lack of two *cis* vacant sites would prevent it from both performing the oxidative addition step and binding the alkene in the *cis* position required for subsequent insertion.

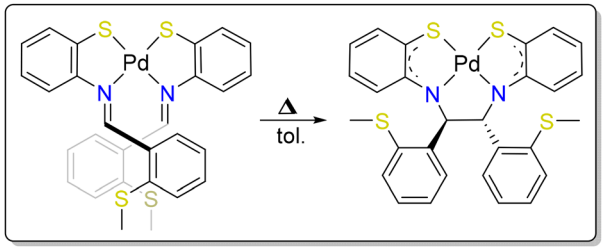

Scheme 2 Isomerization of **Pd-1** to the Pd(N_2S_2) complex.

The ^{1}H NMR spectrum of **Pd-1** at elevated temperature reveals complete transformation into a new species (Fig. S3†), while the ESI-MS spectrum shows the presence of a compound with the same *m*/*z* as **Pd-1** (Fig. S4†), presumably Pd(N_2S_2). This observation supports our hypothesis of the formation of inactive Pd(N_2S_2). To address this issue, we modified our design to incorporate a single SNS ligand. PdI_2 was treated with one equivalent of $(L1)^-$ to afford the four-coordinate complex PdI(κ^3-SNS^{Me}) (**Pd-2**) (Scheme 3). **Pd-2** adopts a slightly distorted square-planar geometry ($\tau'4$ = 0.07). The bond length between Pd1 and S1 is similar to that in **Pd-1** (2.2524(10) Å), while the Pd1–N1 bond in **Pd-2** (2.047(3) Å) is significantly shorter than that in **Pd-1** (2.090(2) Å). The strain in the 5-membered thiolate metallacycle in **Pd-2** [N1–Pd1–S1 = 87.43(9)°], is less than that in **Pd-1** (83.39(7)°), allowing the former to be closer to an ideal square-planar geometry.

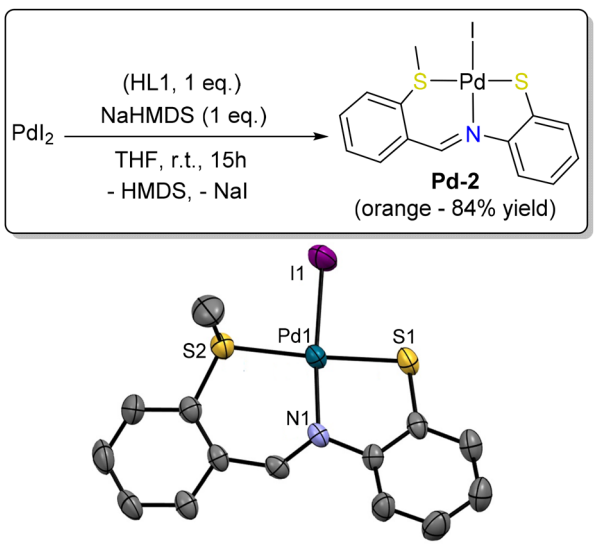

Scheme 3 Synthesis and molecular structure of **Pd-2** showing one of the two independent molecules present in the asymmetric unit. Displacement ellipsoids are drawn at the 50% probability level. The second molecule and all hydrogen atoms have been omitted for clarity. Selected bond distances (Å) and angles (°): Pd1–S1 = 2.2524(10), Pd1–S2 = 2.2930(10), Pd1–N1 = 2.047(3), Pd1–I1 = 2.5834(4), N1–Pd1–I1 = 174.58(9), S1–Pd1–S2 = 175.38(4), N1–Pd1–S1 = 87.43(9), N1–Pd1–S2 = 97.01(9), S1–Pd1–I1 = 87.17(3), S2–Pd1–I1 = 88.40(3).

Table 1 Optimization table for **Pd-2**-catalyzed Heck reaction

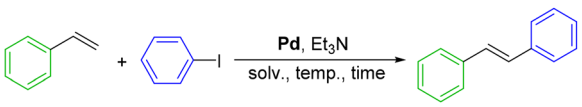

Entry	Cat. (mol%)	Solvent	Time (h)	Temp. (°C)	Yield[a]
1	PdI_2 (5)	DMF	24	120	n.r.
2	**Pd-1** (5)	DMF	24	130	n.r.
3	**Pd-2** (1.5)	DMF	24	120	>99%
4	**Pd-2** (1)	DMF	24	120	84%
5	**Pd-2** (1.5)	C_6H_6	24	Reflux	n.r.
6	**Pd-2** (1.5)	MeCN	24	Reflux	n.r.
7	**Pd-2** (1.5)	MeOH	24	Reflux	n.r.
8	**Pd-2** (1.5)	H_2O	24	Reflux	48%
9[b]	**Pd-2** (1.5)	DMF	24	120	90%
10[c]	**Pd-2** (1.5)	DMF	24	120	n.r.
11[d]	**Pd-2** (1.5)	DMF	24	120	85%
12	**Pd-2** (1.5)	DMF	24	105	>99%
13	**Pd-2** (1.5)	DMF	24	95	87%
14	**Pd-2** (1.5)	DMF	5	105	>99%
15	**Pd-2** (1.5)	DMF	4	105	88%

Reaction conditions: styrene (1 mmol), iodobenzene (1.2 mmol), NEt_3 (2 mmol) in 2 mL of DMF. [a] Isolated yields. [b] Base = Na_2CO_3. [c] Base = KO^tBu. [d] 1.5 mmol of NEt_3.

In contrast to **Pd-1** and PdI_2 which were inactive in the Heck reaction (Table 1, entries 1 and 2), 1.5 mol% of **Pd-2** quantitatively converted the substrates into the desired product (entry 3). However, reducing the catalyst loading to 1 mol% resulted in a decreased yield of 84% (entry 4). Notably, the use of solvents with lower boiling points failed to produce the desired olefin product (entries 5–8), while the reaction achieved nearly half conversion in water (entry 8). Consequently, DMF was selected for subsequent experiments. Among the bases tested, 2 equiv. of triethylamine proved to be the most effective, whereas Na_2CO_3 exhibited lower activity and KO^tBu failed to activate the catalyst (entries 9 and 10). Additionally, using less than 2 equiv. of base adversely affected the reaction yield (entry 11). The optimal reaction temperature was determined to be 105 °C, with an 87% yield observed at 85 °C (entries 12 and 13). Monitoring the reaction over time showed completion within 5 h (entries 14 and 15). With the optimized conditions established, we conducted a small substrate scope study to evaluate the efficiency of **Pd-2** in the Heck reaction. A range of aryl groups bearing electron-donating and electron-withdrawing substituents at different positions was examined (Table 2). Notably, the catalyst failed to produce the desired coupling product when chlorobenzene was used as the substrate. Electron-withdrawing groups at the *ortho* and *para* positions of iodobenzene resulted in quantitative yields (entries a and b). In contrast, the presence of a methyl group at the *para* position reduced the yield to 95% (entry c). Similarly, introducing a methyl group at the *para* position of styrene further decreased the yield to 80% (entry d), while the same substituent at the *ortho* position afforded a quantitative yield (entry e). The introduction of a chloride group at the *para* position also resulted in a quantitative yield (entry f).

Table 2 Substrate scope table for **Pd-2**-catalyzed Heck reaction under optimized conditions

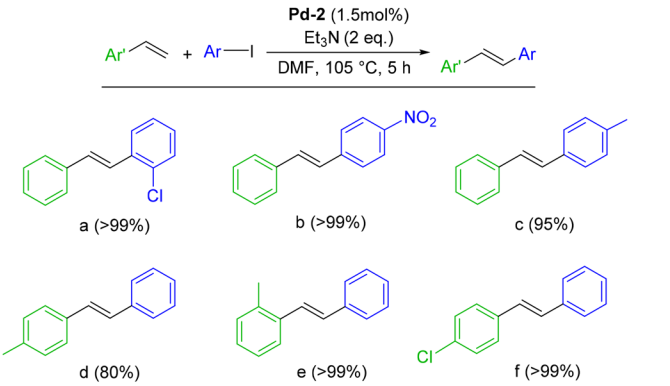

Reaction conditions: alkene (1 mmol), aryl halide (1.2 mmol), Et_3N (2 mmol) in 2 mL of DMF. Isolated yields in parentheses.

To assess the reusability of **Pd-2**, a second batch of starting materials was introduced into the reaction vial following the completion of the initial Heck reaction under standard laboratory conditions. Notably, the results of this subsequent run demonstrated quantitative conversion, highlighting the catalyst's impressive reusability. This outcome further reaffirms the catalyst's robust stability in the presence of environmental factors such as air and moisture. These findings are consistent with similar studies in the field, in which catalysts exhibiting high reusability and stability have proven to be invaluable for sustainable and cost-effective synthetic processes.[24] Additionally, after filtration of the reaction mixture through Celite, no black solid was observed, providing strong evidence for a homogeneous catalytic reaction. This was further confirmed by examining the GC-MS spectra of the filtrate, which showed no evidence of the free protonated thiolate ligand. These observations emphasize the critical role of our thiolate ligand in stabilizing the palladium coordination sphere.

To investigate the activation step and assess catalyst stability under the reaction conditions, we performed stoichiometric NMR experiments. Specifically, we dissolved complex **Pd-2** in DMSO-d_6 with triethylamine, transferred the solution into an NMR tube, and heated it at 120 °C for 24 h. The colour of the solution changed from green to red. The ^1H and ^{13}C NMR spectra were then compared with those of **Pd-2**. The ^1H NMR analysis, shown in Fig. S7,† provided valuable insights. Notably, it revealed the presence of an imine proton, indicating that the thiolate ligand remained coordinated to the metal. This observation supports the idea that the ligand effectively stabilizes the metal complex even under reaction conditions. Furthermore, a closer examination of the ^1H NMR spectrum showed that approximately half of the triethylamine remained unreacted, while the remainder had undergone reaction, leading to the formation of various byproducts in the reaction mixture. Over a period of one month, crystals grew from the reaction mixture. Characterization of these crystals by X-ray crystallography revealed a palladium-dithiolate tetramer in

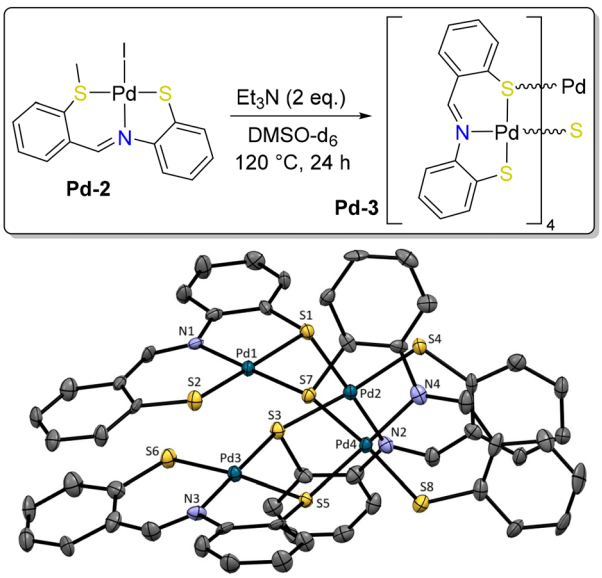

Fig. 2 Synthesis and molecular structure of **Pd-3**·$(C_6H_6)_2$. Displacement ellipsoids are drawn at the 50% probability level. The two benzene solvate molecules and all hydrogen atoms have been omitted for clarity. Selected bond distances (Å) and angles (°): Pd1–S1 = 2.267(2), Pd1–S2 = 2.293(2), Pd1–N1 = 2.059(8), Pd1–S3 = 2.328(2), S1–Pd1–N1 = 95.8(2), S2–Pd1–N1 = 86.1(2), S1–Pd1–S3 = 84.51(8), S2–Pd1–S3 = 94.08(8).

which the five-membered ring thiolate sulfur bridges to a second Pd atom (Fig. 2). The Pd1–S1 bond in **Pd-3** (2.267(2) Å) is within the same range as that in **Pd-1** and **Pd-2**, while the Pd1–N1 bond (2.059(8) Å) is shorter than in **Pd-1** but longer than in **Pd-2**. Notably, the Pd1–S2 bond length in **Pd-3** (2.293 (2) Å), in which the sulfur atom is in the thiolate form and bridges to another Pd center, is identical to the Pd-thioether bond in **Pd-2**. Interestingly, this selective S–C_{Me} bond activation of L1 has been observed previously in Co-[25] and Ni-thiolate[20] complexes, using amido and N-heterocyclic carbene ligands as the base, respectively. In this work, Et_3N is presumed to have caused the activation. Unfortunately, our efforts to regrow the crystal for isolation, further characterization, and catalytic/mechanistic investigation were unsuccessful.

In conclusion, this study makes significant contributions to the broader exploration of SNS-thiolate complexes in Pd-catalyzed, phosphine-free Heck reactions. Complex **Pd-1** did not exhibit reactivity in the Heck reaction, likely due to isomerization into Pd(N_2S_2) (**Pd-3**), highlighting the versatile nature of the redox-active N_2S_2 ligand. While **Pd-2** is not the most efficient catalyst reported for the Heck reaction,[26] its catalytic performance in aqueous solution and its stability as an air-sensitive complex are noteworthy. The fortuitous isolation of the product from the reaction of **Pd-2** with Et_3N led to the discovery of a dithiolate palladium tetramer, in which the thioether arm underwent selective S–C bond activation. This observation complicates the proposal of a definitive mechanism for **Pd-2** in the Heck reaction but provides a valuable foundation for future studies.

Data availability

Electronic Supplementary Information (ESI) available: Selected experimental, structural and spectroscopic data. CCDC 2292482, 2292483 and 2409551.†

Conflicts of interest

There are no conflicts to declare.

Acknowledgements

We thank the NSERC (Discovery Grant 2019-05959) for generous operating support and the University of Ottawa, Canada Foundation for Innovation, and the Ontario Ministry of Economic Development and Innovation for essential infrastructure.

References

1 (*a*) R. F. Heck, *Org. React.*, 1982, **27**, 345–390; (*b*) M. Oestrich, *The Mizoroki–Heck Reaction*, John Wiley & Sons, Ltd, 2009.
2 (*a*) N. Miyaura, K. Yamada and A. Suzuki, *Tetrahedron Lett.*, 1979, **20**, 3437–3440.
3 K. Sonogashira, Y. Tohda and N. Hagihara, *Tetrahedron Lett.*, 1975, **16**, 4467–4470.
4 (*a*) A. O. King, N. Okukado and E. Negishi, *J. Chem. Soc., Chem. Commun.*, 1977, **19**, 683.
5 (*a*) D. Milstein and J. K. Stille, *J. Am. Chem. Soc.*, 1978, **100**, 3636–3638.
6 (*a*) B. Dounay and L. E. Overman, *Chem. Rev.*, 2003, **103**, 2945–2964; (*b*) M. Bagherzadeh, H. Mahmoudi, S. Ataie, M. Bahjati, R. Kia, P. R. Raithby and L. Vaccaro, *Mol. Catal.*, 2019, **474**, 110406.
7 T. Mizoroki, K. Mori and A. Ozaki, *Bull. Chem. Soc. Jpn.*, 1971, **44**, 581.
8 R. F. Heck and J. P. Nolley, *J. Am. Chem. Soc.*, 1972, **37**, 2320–2322.
9 (*a*) C. Eaborn, *J. Organomet. Chem.*, 1995, **490**, C38; (*b*) R. Luan, P. Lin, K. Li, Y. Du and W. Su, *Nat. Commun.*, 2024, **15**, 1723–1733; (*c*) K. Cao, J. Han, H. Shen, J. Yang, J. Zhang and F. Chen, *ACS Catal.*, 2024, **14**, 5305–5313.
10 (*a*) A. d. Meijere and F. E. Meyer, *Angew. Chem., Int. Ed. Engl.*, 1995, **33**, 2379; (*b*) S. Jagtap, *Catalysts*, 2017, **7**, 267; (*c*) W. Li and J. Zhang, *Acc. Chem. Res.*, 2024, **57**, 489–513.
11 (*a*) T. N. Ansari, J. B. Jasinski, D. K. Leahy and S. Handa, *JACS Au*, 2021, **1**, 308–315; (*b*) M. Alisha, R. M. Philip and G. Anilkumar, *J. Organomet. Chem.*, 2022, **959**, 12207; (*c*) A. F. Schmidt, A. A. Kurokhtina, E. V. Larina and N. A. Lagoda, *Organometallics*, 2024, **43**, 1879–1888.
12 (*a*) X. Cui, Z. Li, C. Z. Tao, Y. Xu, J. Li, L. Liu and Q. X. Guo, *Org. Lett.*, 2006, **8**, 2467–2470; (*b*) D. E. Bergbreiter, P. L. Osburn and Y. S. Liu, *J. Am. Chem. Soc.*, 1999, **121**, 9531–9538; (*c*) X. Cui, J. Li, L. Liu and Q. X. Guo, *Chin. Chem. Lett.*, 2007, **18**, 625–628.

13 (*a*) M. R. Elsby and R. T. Baker, *Chem. Commun.*, 2019, **55**, 13574–13577; (*b*) S. Ataie, M. Lohoar, L. P. Mangin and R. T. Baker, *Chem. Commun.*, 2023, **59**, 4044–4046.
14 M. R. Elsby, M. Son, C. Oh, J. Martin, M. H. Baik and R. T. Baker, *ACS Catal.*, 2021, **11**, 9043–9051.
15 S. Ataie, S. Hogeterp, J. A. Ovens and R. T. Baker, *Chem. Commun.*, 2022, **58**, 3795–3798.
16 M. R. Elsby, C. Oh, M. Son, S. Y. H. Kim, M. H. Baik and R. T. Baker, *Chem. Sci.*, 2022, **13**, 12550–12559.
17 M. R. Elsby and R. T. Baker, *Acc. Chem. Res.*, 2023, **56**, 798–809.
18 A. Khanzadeh, S. Ataie and R. T. Baker, *Dalton Trans.*, 2023, **52**, 11768–11772.
19 U. K. Das, S. L. Daifuku, S. I. Gorelsky, I. Korobkov, M. L. Neidig, J. J. Le Roy, M. Murugesu and R. T. Baker, *Inorg. Chem.*, 2016, **55**, 987–997.
20 Y. M. Alkburi, J. S. Oven, J. Martin and R. T. Baker, *Inorg. Chem.*, 2021, **60**, 10934–10942.
21 U. K. Das, C. S. Higman, B. Gabidullin, J. E. Hein and R. T. Baker, *ACS Catal.*, 2018, **8**, 1076–1081.
22 B. Fitchett, MSc thesis, University of Ottawa, 2018.
23 L. P. Mangin, Y. M. Albkuri, J. S. Ovens, S. Al Shehimy, L. Khrouz, S. Steinmann, C. Bucher and R. T. Baker, *Chem. – Eur. J.*, 2024, **30**, e202302714.
24 (*a*) V. Kozell, M. McLaughlin, G. Strappaveccia, S. Santoro, L. A. Bivona, C. Aprile, M. Gruttadauria and L. Vaccaro, *ACS Sustainable Chem. Eng.*, 2016, **4**, 7209–7216; (*b*) A. K. King, A. Brar, G. Li and M. Findlater, *Organometallics*, 2023, **42**, 2353–2358.
25 S. Ataie, S. L. Dudra, E. R. Johnson and R. T. Baker, *ACS Catal.*, 2023, **13**, 10076–10084.
26 (*a*) A. Rajmane and A. Kumbhar, *J. Organomet. Chem.*, 2024, **1012**, 123131; (*b*) P. J. Anju, M. Neetha and G. Anilkumar, *ChemistrySelect*, 2022, **7**, e202103564; (*c*) X.-S. Zhang, Y.-P. Han, Y. Zhang and Y. M. Liang, *Adv. Synth. Catal.*, 2023, **365**, 2436–2466.